The Scaling of Relaxation Processes—Revisited

Friedrich Kremer and Alois Loidl

Abstract Glassy dynamics covers the extraordinary spectral range from 10^{+13} to 10^{-3} Hz and below. In this broad frequency window, four different dynamic processes take place: (i) the primary or α-relaxation, (ii) (slow) secondary relaxations (β-relaxations), (iii) fast absorption processes in the GHz and (iv) the boson-peak in the THz range. The dynamic glass transition is assigned to fluctuations between structural substates and scales well with the calorimetric glass transition temperature. It shows a similar temperature dependence as the viscosity and fluctuations of the density or heat capacity. The temperature dependence of the mean relaxation rate of the dynamic glass transition follows at first glance the empirical Vogel–Fulcher—Tammann law, albeit a further analysis unravels clear-cut deviations. The (slow) secondary relaxations are assigned to librational relaxations of molecular subgroups hence having a straightforward molecular assignment. They may also show up as a wing on the high-frequency side of the dynamic glass transition. The fast absorption processes at GHz frequencies can formally be described within the framework of the mode-coupling theory (MCT). The boson-peak resembles the Poley absorption and originates from overdamped oscillations. In this chapter, especially the first three contributions will be discussed in detail and compared with existing theoretical models.

F. Kremer (✉)
Molekülphysik, Peter-Debye-Institut für Physik der weichen Materie, Universität Leipzig, Linnéstr. 5, 04103 Leipzig, Germany
e-mail: kremer@physik.uni-leipzig.de

A. Loidl
University of Augsburg, Experimental Physics V, Universitätsstrasse 2, 86135 Augsburg, Germany
e-mail: alois.loidl@physik.uni-augsburg.de

F. Kremer and A. Loidl (eds.), *The Scaling of Relaxation Processes*,
Advances in Dielectrics, https://doi.org/10.1007/978-3-319-72706-6_1

1 Introduction

The glassy state is ubiquitous in inorganic and organic matter. It is characterized by the lack of long range order and shows a refined dynamics including processes spanning a spectral range from 10^{+13} to 10^{-3} Hz and below. Despite concentrated efforts [1–9], a common theoretical understanding of the glassy state does not exist and a variety of different and often controversial views compete. The glassy state is furthermore reflected in many different physical quantities, e.g. the heat capacity, the viscosity, the mechanical moduli, the density, ultrasonic absorption, magnetization, the complex index of refraction and the complex dielectric function. Hence, a multitude of experimental techniques have been employed to study glassy materials, such as frequency-dependent and differential scanning calorimetry [10], dynamic mechanical spectroscopy [11], ultrasound attenuation [12], light [13] and neutron scattering [14], NMR spectroscopy [15] and especially broadband dielectric spectroscopy [16–38].

The mean relaxation rate $\nu(T)$ of the α-relaxation is characterized by the empirical Vogel–Fulcher–Tammann (VFT)-equation [39–41]:

$$\nu(T) = \frac{1}{2\pi\tau(T)} = \upsilon_\infty \exp\left[\frac{-DT_0}{T - T_0}\right] \tag{1}$$

where $\upsilon_\infty = (2\pi\tau_\infty)^{-1}$ is the high temperature limit of the relaxation rate, D is a constant, and T_0 denotes the Vogel–Fulcher temperature. The "fragility" parameter D [42] describes hereby the deviation from an Arrhenius-type temperature dependence

$$\nu(T) = \nu_\infty \exp\left(\frac{-E_A}{kT}\right) \tag{2}$$

where E_A is the activation energy and k the Boltzmann constant. At the calorimetric glass transition T_g, the mean relaxation rate $\nu(T_g)$ and the viscosity $\eta(T_g)$ have reached typical values of ~10^{-3} Hz and ~10^{13} Poise, respectively. In general, T_0 is found to be approximately 40 K below T_g. Thus, the change in the dynamics of the glass-forming processes spans more than 15 decades.

The divergence of Eq. (1) at $T = T_0$ is also supported by the so-called Kauzmann paradox occurring in the entropy determined by measurements of the specific heat [43, 44]: if the entropy of the supercooled liquid is extrapolated to low temperatures, it seems to become identical to that of a crystal or even smaller. In some theories (like the Gibbs–Di Marzio model [45] for polymers), the Kauzmann paradox is resolved by a phase transition. But the physical meaning of the divergence of $\nu(T)$ at $T = T_0$ remains unclear. Because of the universality of Eq. (1), T_0 is considered as a characteristic temperature, where the mean relaxation rate extrapolates to zero, albeit little evidence could be found for a dynamic divergence [46].

Qualitatively, glassy dynamics is often discussed as fluctuation of a molecule in the cage of its neighbours. The librational motions of the latter give rise to fast secondary β-relaxations which take place on a time scale of 10^{-10}–10^{-12} s, while the

reorientations of the molecules forming the cage are assigned to the dynamic glass transition or α-relaxation obeying a VFT-temperature dependence. This relaxation process must have cooperative character; i.e. the fluctuations of the molecules forming the "cage" cannot be independent from each other. The extension of the size of such "cooperatively rearranging domains" [3, 6, 7, 45] is one of the central (and controversial) topics of glass research.

The relaxation function of the α-relaxation is usually broadened. Its high-frequency side exhibits often two power laws. In the case of glycerol, this was observed already by Davidson and Cole [47] and interpreted as caused by high-frequency vibrations. It is nowadays established for a variety of glass-forming (low molecular weight and polymeric) materials [s. also the chapter of P. Lunkenheimer and A. Loidl and F. Kremer et al. in this book] and considered to be the high-frequency contribution of a secondary relaxation.

Many systems show additionally a slow secondary β-relaxation (with an Arrhenius-type temperature dependence). This process being observed for relaxation rates $\sim<10^8$ Hz can often be assigned to intramolecular fluctuations. But there are several examples like the low molecular weight liquid ortho-terphenyl (OTP) [19, 20] or the main chain polymer poly(ethylene terephthalate) (PET) [38] where such an interpretation is not immediately obvious. Therefore, it was suggested by Goldstein and Johari [11, 12] that the slow β-relaxation "is intrinsic to the nature of the glassy state" [12]. In the THz regime a further molecular process is observed, the "boson peak" [4] which has similarities with the Poley absorption [48], which was interpreted as being caused by strong local fields exerted on a molecule by its immediate neighbours in the glassy state (Fig. 1).

In detail in this chapter, the following questions will be addressed: (i) is there a scaling function which describes the temperature dependence of the mean relaxation rate in the entire spectral range from 10^{+11} to 10^{-3} Hz and below? (ii) How does the relaxation time distribution function change with temperature, or in other words, is time–temperature superposition in general valid for (dielectric) relaxation processes? (iii) How does the strength $\Delta\varepsilon$ of a relaxation process change with temperature in the course of the dynamic glass transition? (iv) What is the molecular origin of the "high-frequency" wing, sometimes termed excess wing, which is observed in the dynamic glass transition of many (low molecular weight and polymeric) systems? (v) Is there a model-free characteristic temperature, where glassy dynamics undergoes a change?

2 Theories Describing the Scaling of Relaxation Processes in Glassy Systems

Numerous approaches [49–69] have been developed to describe the dynamics of glassy systems. In the following, two most important approaches are briefly described.

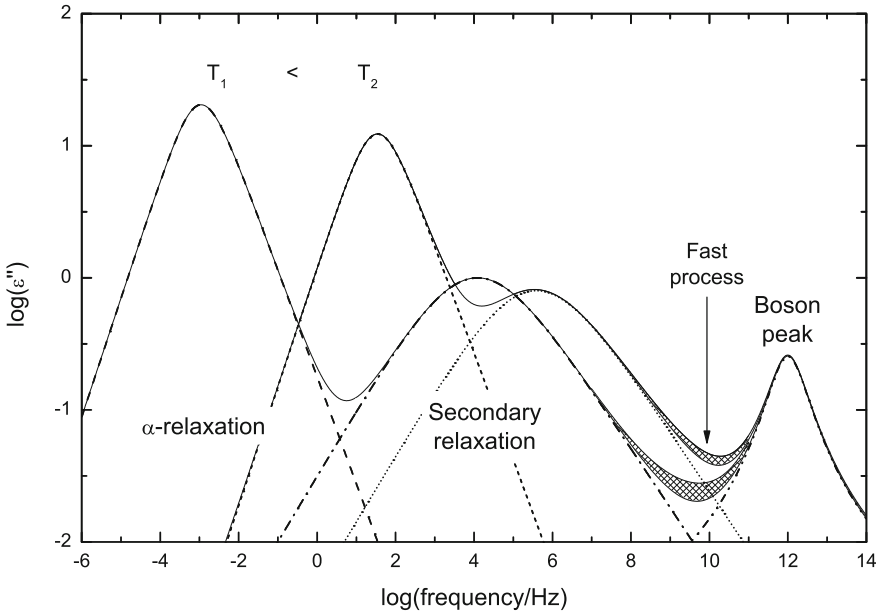

Fig. 1 Scheme of the dynamical processes taking place in the spectral range between 10^{-6} and 10^{14} Hz, (i) the α-relaxation, (ii) (slow) secondary relaxations, (iii) fast absorption processes and (iv) the boson peak. The temperature shift is depicted for two different temperatures $T_1 < T_2$

The experimentally observed VFT-dependence (Eq. (1)) can be founded by two approaches: the Adam–Gibbs model [52] and the free volume theory as developed by Doolittle [53] and Cohen and Turnbull [54, 55]. The latter is based on four assumptions:

(i) A local volume V is attributed to a molecule or polymer segment.
(ii) The difference $V_f = V - V_c$ can be considered as "free", if V is larger than a critical value V_c.
(iii) If for the free volume $V_f \geq V^* \approx V_M$ holds, molecular transport takes place in jumps over a distance corresponding to the size of the molecule V_M. V^* is the minimal free volume required for a jump of a molecule.
(iv) The molecular rearrangement of free volume does not require free energy.

Following Boltzmann statistics, a molecule or a polymer segment carries out positional jumps only if the necessary free volume is provided. Hence for the jump rate $1/\tau$

$$\frac{1}{\tau} \sim \int_{V^*}^{\infty} \exp\left[-\frac{V_f}{V_f}\right] dV_f \sim \exp\left[-\frac{V^*}{V_f}\right]. \tag{3}$$

is obtained where $\overline{V}_f$ is the averaged free volume. Assuming that the relative averaged free volume $\bar{f} = \overline{V}_f / V$ (V: total volume) depends linearly on temperature

$$\bar{f} = f_g + \alpha_f (T - T_g) \tag{4}$$

while $f^* = \frac{V^*}{V}$ is temperature-independent results in a VFT-equation. α_f is the thermal expansion coefficient of the free volume and f_g the relative free volume at T_g. Comparison with Eq. (1) delivers

$$DT_0 = \frac{f^*}{\alpha_f}, \quad T_0 = T_g - \frac{f_g}{\alpha_f} \tag{5}$$

At the temperature T_0, the volume $\overline{V}_f$ vanishes. Within this approach, no inherent length scale is involved and all transport properties should have the same temperature dependence because the jump between holes is the only transport mechanism. Cohen and Grest [55] extended this approach by considering solid- and liquid-like clusters in a percolation approach.

The model of Adam and Gibbs [52] suggests the existence of "Cooperatively Rearranging Regions (CRR)" being defined as the smallest volume which can change its configuration independent from neighbouring regions. It relates the relaxation time to the numbers of particles (molecules for a low molecular liquid, segments for a polymer) $z(T)$ per CRR by

$$\frac{1}{\tau} \sim \exp\left[-\frac{z(T)\,\Delta E}{k\,T} \right] \tag{6}$$

where ΔE is a free energy barrier for one molecule. $z(T)$ can be expressed by the total configurational entropy $S_c(T)$ as $z(T) = S_c(T)/(N\ k_B\ \ln 2)$ where N is the total number of particles, k_B the Boltzmann constant and ln 2 the minimum entropy of a CRR assuming a two-state model. Using thermodynamic considerations, $S_c(T)$ can be linked to the change of the heat capacitance Δc_p at the glass transition by

$$S_c(T) = \int_{T_2}^{T} \frac{\Delta c_p}{T}\, dT \tag{7}$$

With $T_2 = T_0$ and $\Delta c_p \approx C/T$ from Eqs. (6) and (7), the VFT-dependence follows. At T_0, the configurational entropy vanishes and the size of a CRR diverges as $z(T) \sim \frac{1}{C(T-T_0)}$. The Adam–Gibbs model does not provide information about the absolute size of the CRR at T_g.

Donth [3, 6, 7] suggested a thermodynamic fluctuation model leading to a expression which connects the height of the step in c_p and the temperature fluctuation δT of a CRR at T_g with the correlation length ξ as

$$\xi^3 \sim V_{\mathrm{CRR}} = \frac{k\, T_g^2 \Delta(1/c_p)}{\rho(\delta T)^2}. \tag{8}$$

where ρ is the density and $\Delta(1/c_p)$ the step of the reciprocal specific heat (if $c_V \approx c_p$ is assumed). Experimentally, δT can be extracted from the width of the glass transition [6, 7] or from thermal heat spectroscopy measurements [56, 57].

Within the fluctuation approach for the temperature dependence of ξ

$$\xi(T) \sim \frac{1}{(T - T_0)^{2/3}} \tag{9}$$

is obtained. A similar equation was derived by Kirkpatrick and Tirumalai [58] using scaling arguments.

Based on the Adam–Gibbs equation (6) and an expression proposed by Waterton [59] as early as 1932, Mauro et al. [60] suggested an approach, which avoids the divergence of the VFT-formula (1) at $T = T_0$

$$\nu(T) = \nu_\infty \exp\left[\frac{K}{T} \exp\left(\frac{C}{T}\right)\right] \tag{10}$$

K and C are related to activation energies deduced through a "physical realistic model for configurational entropy based on a constraint approach".

In comparing viscous liquids with spin glasses, Souletie and Bertrand [61] suggested for the mean relaxation rate

$$\tau^{-1} \sim \left[\frac{(T - T_c)}{T}\right]^\gamma \tag{11}$$

where $\gamma > 0$ and T_c are constants.

The shoving model developed by Dyre et al. [62] is based essentially on three assumptions.

1. The activation energy is mainly elastic energy.
2. This elastic energy is mainly located in the surroundings of the flow event.
3. The elastic energy is mainly shear elastic energy.

It relates the mean relaxation rate to the mean square vibrational displacement $\langle u^2 \rangle(T)$ and a characteristic molecular length a, which is assumed to be constant.

$$\nu(T) = \nu_\infty \exp\left(-\frac{a^2}{\langle u^2 \rangle(T)}\right) \tag{12}$$

In [63, 64], it is shown that the temperature dependence of the shear modulus dominates the temperature dependence, leading to

$$\langle u^2 \rangle(T) \propto \frac{T}{G_\infty(T)} \tag{13}$$

where $G_\infty(T)$ is the elastic shear modulus. The shoving model does not make a specific prediction of the temperature dependence of the mean relaxation rate, except that it cannot diverge at any finite temperature. The model, however, relates two independently measurable quantities in a prediction that has been confirmed for several glass-forming liquids; see for example, the review of the experimental situation given in [65].

The mode-coupling theory (MCT) [9, 66–69] is a hard sphere model based on a generalized nonlinear oscillator equation

$$\frac{\mathrm{d}^2\Phi_\mathrm{q}(t)}{\mathrm{d}t^2} + \Omega^2\Phi_\mathrm{q}(t) + \zeta\frac{\mathrm{d}\,\Phi_\mathrm{q}(t)}{\mathrm{d}t} + \Omega^2\int_0^t m_\mathrm{q}(t-\tau)\frac{\mathrm{d}\,\Phi_\mathrm{q}(\tau)}{\mathrm{d}\tau}\mathrm{d}\tau = 0 \qquad (14)$$

where $\Phi(t)_\mathrm{q}$ is the normalized density correlation function defined as

$$\Phi_\mathrm{q}(t) = \frac{\left\langle \Delta\rho_q(t)\Delta\rho_\mathrm{q}(0)\right\rangle}{\left\langle \Delta\rho_\mathrm{q}^2\right\rangle} \qquad (15)$$

$\Delta\rho_\mathrm{q}(t)$ are density fluctuations at a wavevector q, Ω is a microscopic oscillator frequency, and ς describes a frictional contribution. The first three terms of Eq. (14) describe a damped harmonic oscillator; the fourth term contains a memory function $m_\mathrm{q}(t-\tau)$. As a consequence, the total frictional losses in the system become time-dependent.

In order to solve Eq. (14), an ansatz for $m_\mathrm{q}(t)$ is required. Already a simple Taylor expansion of m leads to a relaxational response of Φ_q having some similarity with the dynamic glass transition [66, 67]. Assuming $m_\mathrm{q}(t) = v_1\Phi_\mathrm{q}(t) + v_2\Phi_\mathrm{q}^2(t)$ (F_{12}-model, [67]) delivers a two-step decrease of the correlation function $\Phi_\mathrm{q}(t)$. The faster contribution is interpreted in terms of a (fast) β-relaxation while the slower component to the dynamic glass transition (α-relaxation). At a critical temperature T_c, the relaxation time diverges; this is interpreted as a phase transition from an ergodic ($T > T_\mathrm{c}$) to a non-ergodic ($T < T_\mathrm{c}$). Furthermore, MCT (in the idealized version) makes the following predictions:

(i) for $T > T_\mathrm{c}$ the relaxation time τ_α of the α-relaxation scales according to

$$\tau_\alpha \sim \eta \sim \left[\frac{T_\mathrm{c}}{T - T_\mathrm{c}}\right]^\gamma \qquad (16)$$

where γ is a constant.

(ii) the relaxation function of the α-relaxation can be described by

$$\Phi_\mathrm{q}(t) \sim \exp\left[-\left(\frac{t}{\tau_\alpha}\right)^{\beta_\mathrm{KWW}}\right] \qquad (17)$$

with $(0<\beta_{\mathrm{KWW}}<1)$, where Φ_0 is the amplitude of the α-relaxation. For $T>T_c$, the relaxation time distribution should be temperature-independent; i.e. time–temperature superposition should hold.

(iii) above and close to the critical temperature T_c, the minimum of the susceptibility $\left(\varepsilon''_{\min},\ \omega_{\min}\right)$ between the α-relaxation and the β-relaxation should follow a power law

$$\varepsilon''_{\min} \sim \left|\frac{T-T_c}{T_c}\right|^{1/2} \tag{18}$$

Glassy dynamics spans a time scale of more than 15 decades. In order to unravel the evolution of the temperature dependence in detail, it is most advantageous to calculate the derivatives of the mean relaxation rate with respect to 1/T of the different theoretical approaches. By that, one obtains for the VFT-equation (Eq. (1)) the Arrhenius dependence (Eq. (2)), the Mauro equation (Eq. (10)), the approach by Souletie and the MCT (Eq. (11)) for $T>T_c$ the following expressions:
VFT:

$$\frac{\mathrm{d}\log\nu}{\mathrm{d}(1/T)} = -(DT_0)\cdot\log e\cdot\left(1-\frac{T_0}{T}\right)^{-2} \tag{19}$$

Arrhenius:

$$\frac{\mathrm{d}\log\nu}{\mathrm{d}(1/T)} = \frac{-E_A}{k}\cdot\log e \tag{20}$$

Mauro:

$$\frac{\mathrm{d}\log\nu}{\mathrm{d}(1/T)} = K\cdot\log e\cdot\exp\left(\frac{C}{T}\right)\cdot\left(\frac{C}{T}+1\right) \tag{21}$$

Souletie:

$$\frac{\mathrm{d}\log\upsilon}{\mathrm{d}(1/T)} = \gamma\cdot\log e\cdot\frac{T_C\cdot T}{T_c-T} \tag{22}$$

MCT:

$$\frac{\mathrm{d}\log\upsilon}{d(1/T)} = \gamma\cdot\log e\cdot\frac{T^2}{T_C-T} \tag{23}$$

Hence in a plot of the *differential* quotient $\mathrm{d}(-\log\nu/\mathrm{d}(1/T))^{-1/2}$ versus $1/T$, the VFT-dependence shows up as a straight line. The derivative plots enable to analyse in detail the scaling with temperature (Fig. 2). This is especially true for the high temperature regime. By that the *difference* quotient, $\Delta(-\log\nu)/\Delta(/1/T)$ of the experimental data can be determined and compared with the analytical derivatives.

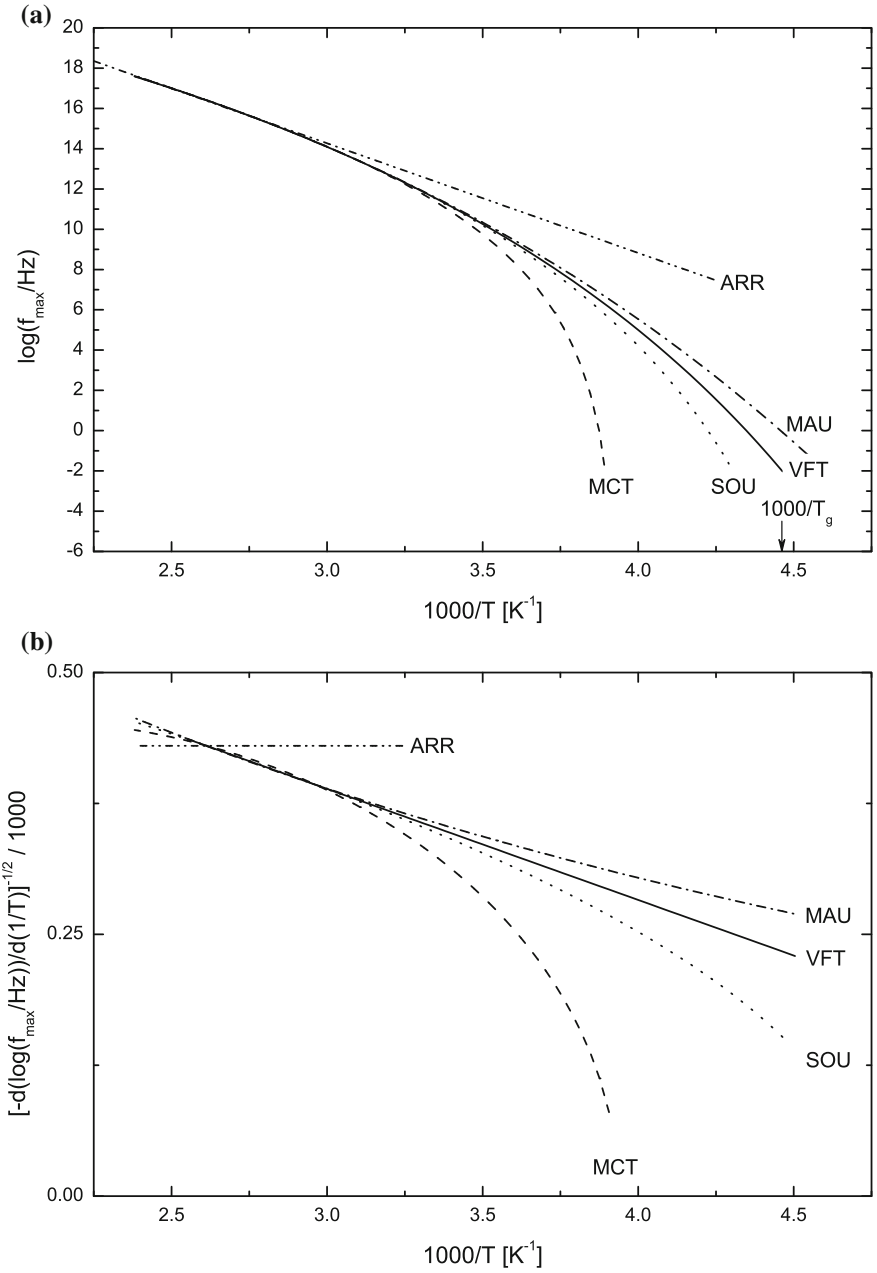

Fig. 2 **a** The scaling behaviour as predicted by the Arrhenius equation (Eq. 2), the Vogel-Fulcher-Tammann equation (VFT) (Eq. 1), the Mauro approach (Eq. 10), that of Souletie (Eq. 11) and of the mode-coupling theory (MCT) (Eq. 16). The glass transition temperature Tg as the temperature, where the mean relaxation rate according to the VFT-function has reached a value of 10^{-2} Hz is indicated. **b** Differential quotient $(-\mathrm{d}(\log(\nu)/(\mathrm{d}(1/\mathrm{T}))^{-1/2} \times 100$ for the functionalities shown in **a**

3 The Scaling of the Dynamic Glass Transition in Low Molecular Weight and Polymeric Organic Glasses

Salol is one of the most explored organic glass-forming liquids. It is considered as a van der Waals glass, despite the fact that it can form H-bonds, presumably mainly within the same molecule. In Fig. 3, dielectric measurements [70] extended over a broad spectral range from about 10^{-2} Hz up to 10^{11} Hz are displayed for temperatures 211 and 361 K. The charts are characterized by a pronounced dynamic glass transition (α-relaxation) having an excess wing, which appears as a second power law on the high-frequency flank of the α-relaxation [71]. The latter is interpreted as a submerged slow secondary relaxation showing up as a shoulder with a significant curvature for a sample aged at 211 K for 6.5 days as discussed in detail in ref. [72]. For frequencies $\nu > 10^{10}$ Hz, a shallow loss minimum is found; it can be interpreted in terms of the fast β-relaxation of the mode-coupling theory (s. below) but also other explanations have been proposed [73].

The spectra can be described by a superposition of a Havriliak–Negami (HN) and Cole–Cole (CC) [16] function for the primary α-process or for the secondary β-process, respectively:

$$\varepsilon^*_{total}(\omega) = \varepsilon_\infty + \frac{\Delta\varepsilon_{\mathrm{HN}}}{(1+(i\omega\,\tau_{\mathrm{HN}})^{\beta_{\mathrm{HN}}})^{\gamma_{\mathrm{HN}}}} + \frac{\Delta\varepsilon_{\mathrm{CC}}}{(1+(i\omega\,\tau_{\mathrm{CC}})^{\beta_{\mathrm{CC}}})} \tag{24}$$

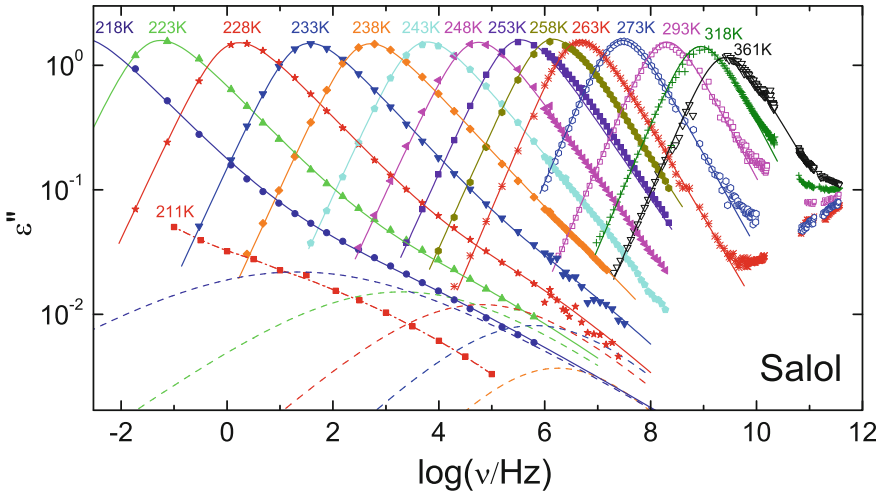

Fig. 3 Dielectric loss as a function of frequency for a series of temperatures from 211 K up to 361 K for salol. The solid lines are fits with a Havriliak–Negami (HN) function for $T \geq 243$ K and with the sum of a HN and Cole–Cole (CC) function for $T \leq 238$ K. The dashed lines show the CC components. The dash-dotted line through the 211 K data is a guide to the eyes. Taken and modified from [70] with kind permission of The European Physical Journal (EPJ)

where $\Delta\varepsilon_{HN}$ and $\Delta\varepsilon_{CC}$ are the relaxation strengths, τ_{HN} and τ_{CC} the relaxation times, and β_{HN}, γ_{HN} and β_{CC} the spectral width parameters of the HN and CC function, respectively, and ω is the circular frequency. For temperatures $T \geq 243$ K, the secondary β-peak has completely merged with the α-peak.

By fitting the dielectric spectra with the empirical relaxation function of Eq. (24), an activation plot is obtained, where the mean relaxation rate versus the inverse temperature is displayed (Fig. 4a). The charts at temperatures >300 K can be equally well described by the Arrhenius equation, the formula suggested by Mauro (Eq. (10)) and Souletie (Eq. (11)) and the MCT-ansatz (Eq. (16)). Comparing the experimentally determined difference quotients with the derivatives of the different scaling functions with respect to 1/T however proofs that *none* of the suggested formulae describes the data within the limits of experimental accuracy in the entire temperature range and that it is furthermore *not* possible to describe the experimental data adequately by use of *one* VFT-function or to replace the VFT-dependence by an Arrhenius function as one might expect from the raw data in Fig. 4a. This is supported as well by an analysis [74] based on the second derivative of the temperature dependence of the structural relaxation time $\tau_\alpha(T)$ with respect to T_g/T.

Glycerol (Fig. 5a/b) is an H-bond forming liquid. Its mean relaxation rate shows a pronounce VFT-dependence; the data for temperatures ≥ 270 K seem to follow equally well a VFT-function or dependencies as suggested by Mauro, Souletie or the MCT. But from the derivative plot (Fig. 5b) again one must conclude that none of the suggested formulae fits the temperature dependence correctly within the limits of experimental accuracy. Similarly as for salol, two VFT-equations (VFT1 and VFT2) are required to describe the data within experimental accuracy in the entire temperature range. From the derivative plots, it can be deduced that at temperatures above 270 K neither the Arrhenius equation nor the MCT-ansatz is adequate.

The dynamic glass transition for propylene glycol, tripropylene glycol and its polymeric counterpart poly(propylene glycol) having a mean molecular weight of $M_w = 4000$ g/mol are compared in Fig. 6a. Both charts display a VFT-dependence, but due to the connectivity of the chain for the latter the relaxation is slower, especially at lower relaxation rates. In the derivative plots (Fig. 6b), it is shown again that a single VFT-dependence is *not* sufficient to describe the data adequately in the entire temperature range.

A dielectric relaxation process is not only characterized by the relaxation rate but also by its dielectric strength and by the shape of the relaxation time distribution function. According to the Debye formula, the product $T\Delta\varepsilon$ should be independent on temperature besides the weak temperature effect on number density of dipoles. Instead one observes (Fig. 7a) for all materials that $T\Delta\varepsilon$ increases with decreasing temperature; this might be interpreted as caused by a growing length scale, where polar fluctuations become more cooperative and hence its *effective* dipole moment increases. The temperature dependencies suggested by the MCT $T\Delta\varepsilon \sim (T_c - T)^{1/2}$ for $T < T_c$ and $T \times \Delta\varepsilon \approx$ const. for $T > T_c$ are not fulfilled. However, one has to be aware that the reported values of delta epsilon in most cases exhibit large experimental uncertainties and sometimes differ considerably when reported by different

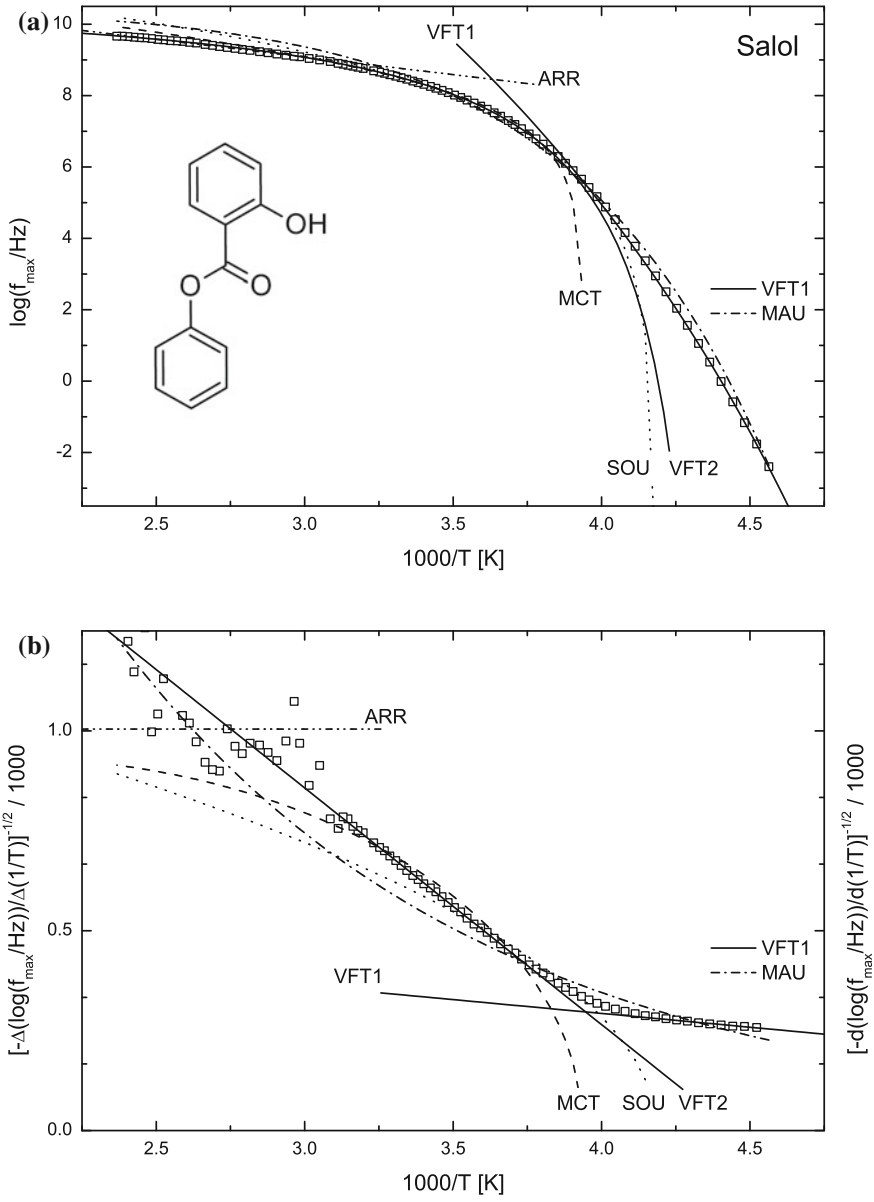

Fig. 4 **a** Activation plot for salol. *Solid lines*: VFT-fits (VFT1): $\log\nu_\infty = 23.5$, $DT_0 = 4618$ K, $T_0 = 141.6$ K; (VFT2) $\log\nu_\infty = 10.4$, $DT_0 = 333$ K, $T_0 = 224.7$ K. *Dash double dotted line*: Arrhenius-fit $\log\nu_\infty = 12.1$, $E_A/k_B = 2283$ K. *Dashed line*: MCT fit $\log\nu_\infty = 10.4$, $\gamma = 2.6$, $T_c = 254$ K; *dotted line*: Souletie fit $\log\nu_\infty = 12.1$, $\gamma = 5.25$, $T_c = 239$ K; *dash-dotted line*: Mauro fit $\log\nu_\infty = 10.5$, $K = 17.1$ K, $C = 1301$ K. The data are taken from [37b, 75]; the error bars are smaller than the size of the symbols if not indicated otherwise. **b** Difference quotient $(-\Delta(\log(\nu_{max}))/\Delta(1000/T))^{-1/2}$ versus 1000/T for the data shown in **a**. For comparison, the differential quotients for the VFT-equation and the temperature dependencies as suggested by the mode-coupling theory (MCT), Souletie (SOU), and Mauro theory (MAU) using the fit parameters shown in **a**

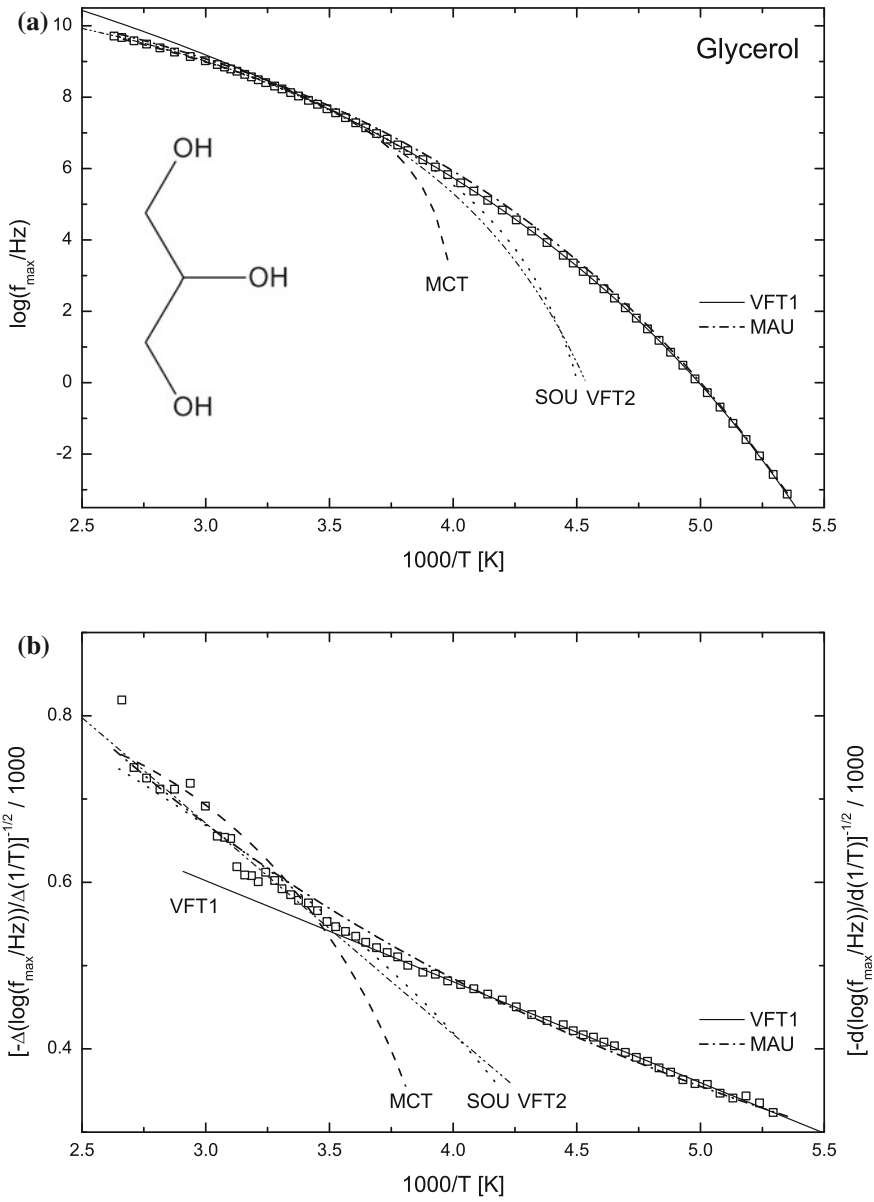

Fig. 5 **a** Activation plot for glycerol. *Solid line*: VFT-fit (VFT1): $\log\nu_\infty = 14.3$, $DT_0 = 2448$ K, $T_0 = 126.0$ K. *Dash double dotted*: VFT-fit (VFT2): $\log\nu_\infty = 12.0$, $DT_0 = 1331$ K, $T_0 = 183.1$ K. *Dashed line*: MCT fit with $\log\nu_\infty = 10.4$, $\gamma = 3.65$, $T_c = 248.8$ K. *Dotted line*: Souletie fit with $\log\nu_\infty = 12.8$, $\gamma = 3.69$, $T_c = 215.1$. *Dash-dotted line*: Mauro fit with $\log\nu_\infty = 12.8$, $K = 517$ K, $C = 471$ K. Data taken from [37b, 75]. The *error bars* are smaller than the size of the symbols if not indicated otherwise. **b** Experimentally determined difference quotient $(-\Delta(\log(\nu_{\max}))/\Delta(1000/T))^{-1/2}$ versus $1000/T$. The lines describe the fits shown in **a**. For comparison, the differential quotients for the VFT-fits and the temperature dependencies as suggested by the mode-coupling theory (MCT), Souletie (SOU), and Mauro (MAU) theory using the fit parameters shown in **a**

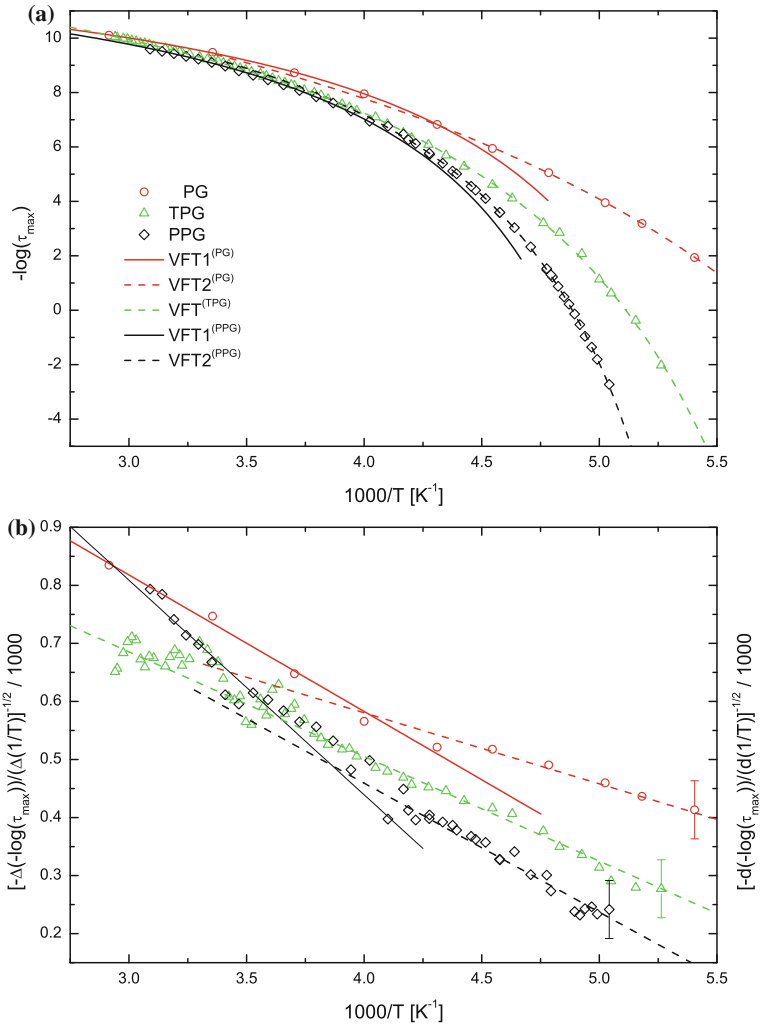

Fig. 6 **a** Activation plot for propylene glycol (open circles), tripropylene glycol (open triangles) and the polymeric pendant ($M_w = 2000$ g/mol) poly(propylene glycol) (open diamonds). The error bars are smaller than the size of the symbols if not indicated otherwise. Solid lines (VFT_1): VFT-fits with $\log\nu_\infty = 12.1$, $DT_0 = 793$ K, $T_0 = 166$ K for propylene glycol and $\log\nu_\infty = 12.1$, $DT_0 = 833$ K, $T_0 = 179$ K for poly(propylene glycol)). Dashed lines (VFT_2): VFT-fits for the lower temperature range with $\log\nu_\infty = 14.1$, $DT_0 = 1956$ K; $T_0 = 115$ K for propylene glycol, $\log\nu_\infty = 13.1$, $DT_0 = 1343$ K; $T_0 = 151$ K for tripropylene glycol, and $\log\nu_\infty = 12.8$, $DT_0 = 1041$ K, $T_0 = 169$ K for polypropylene glycol. **b** Difference quotient $(-\Delta(\log(\nu_{max}))/\Delta(1000/T))^{-1/2}$ versus $1000/T$. For comparison the differential quotients for the VFT-fits using the fit parameters from **a** are depicted. The data for propylene glycol and poly(propylene glycol) are taken from [16] and for tripropylene glycol from [75]

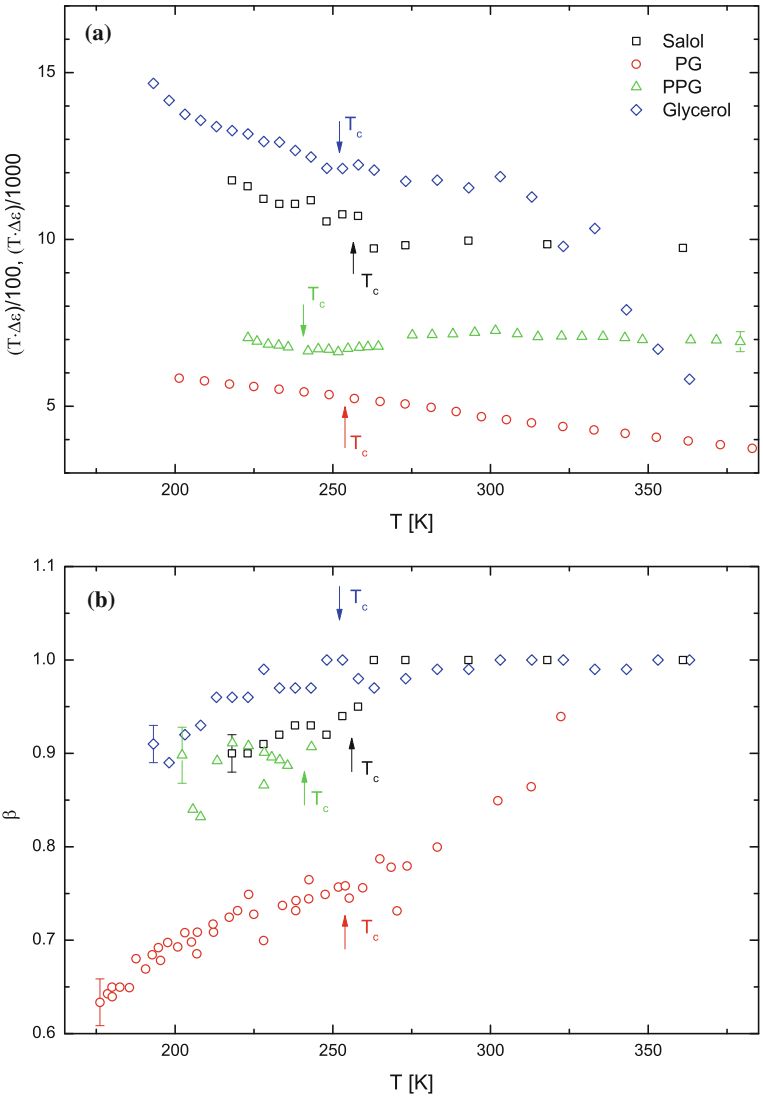

Fig. 7 **a** The product of relaxational strength $\Delta\varepsilon$ and temperature T, $(T\Delta\varepsilon)$ versus T; for salol, propylene glycol (PG), poly(propylene glycol) (PPG) and glycerol as indicated. For salol and PPG, $T\Delta\varepsilon$ is normalized by 100 and for PG and glycerol by 1000. The error bars are smaller than the size of the symbols if not indicated otherwise. The critical temperatures Tc of the MCT are indicated for the different materials. The data for salol are taken from [76], for PG from [16], for PPG from [77] and for glycerol from [78]. **b** Shape parameter β from the Cole–Davidson function for the materials shown in **a**

groups. There are also some reports which show at least a rough agreement with the predictions of MCT [76].

For all examined materials shown in Fig. 7b, the shape parameter β of the Cole—Davidson function shows a strong temperature dependence. This holds in general for the vast majority of glass-forming (low molecular weight and polymeric) materials and proves that relaxation processes do *not* obey the rule of time–temperature superposition which is often employed in mechanical spectroscopy.

Schönhals [79] analysed the scaling of the dynamic glass transition for a variety of glassy materials and suggested to display the two *measured* quantities, the relaxation strength versus the mean relaxation rate. By that, he found unambiguously that as different materials as salol, glycerol, propyleneglycol, dipropylenglycol, tripropylenglycol and poly(propylene glycole), a pronounced change in the slope of the correlation between the two dependent quantities exists. This crossover takes place at a mean relaxation rate of about 10^8 Hz and marks perhaps the beginning of cooperative dynamics. For all materials, the relaxation strength increases strongly with decreasing temperature. Extrapolated to high temperatures, the mean relaxation rate is in the range between 10^{11} and 10^{13} Hz which is typical for highly activated librational fluctuations. The fact that a crossover temperature T_B exists can be interpreted in several ways; (i) T_B and the critical temperature T_c of the MCT have some resemblance, hence the crossover might reflect a transition from an ergodic to a non-ergodic state. (ii) T_B can be also comprehended as the onset of a cooperative dynamics as suggested by Donth [6, 7]. It is characterized by cooperatively rearranging domains having a size $\xi(T)$ which increases with decreasing diameter. At the calorimetric glass transition temperature T_g, a value between 2 and 3 nm can be estimated based on multiple studies [80] of glassy dynamics in nanometric confinement (Fig. 8).

The mode-coupling theory makes detailed predictions for the minimum region between the "microscopic peak" and the dynamic glass transition following a master function:

$$\varepsilon''(\omega) = \frac{\varepsilon''_{\min}}{a+b}\left[b\left(\frac{\omega}{\omega_{\min}}\right)^a + a\left(\frac{\omega_{\min}}{\omega}\right)^b\right] \tag{25}$$

with temperature-independent exponents a and b being interrelated as

$$\frac{\Gamma^2(1+b)}{\Gamma(1+2b)} = \lambda = \frac{\Gamma^2(1-a)}{\Gamma(1-2a)} \tag{26}$$

where Γ is the Γ-function. The exponents can be as well determined from the temperature dependence of the frequency of the minimum of the susceptibility and of the frequency of the maximum ω_{max} of the dynamic glass transition

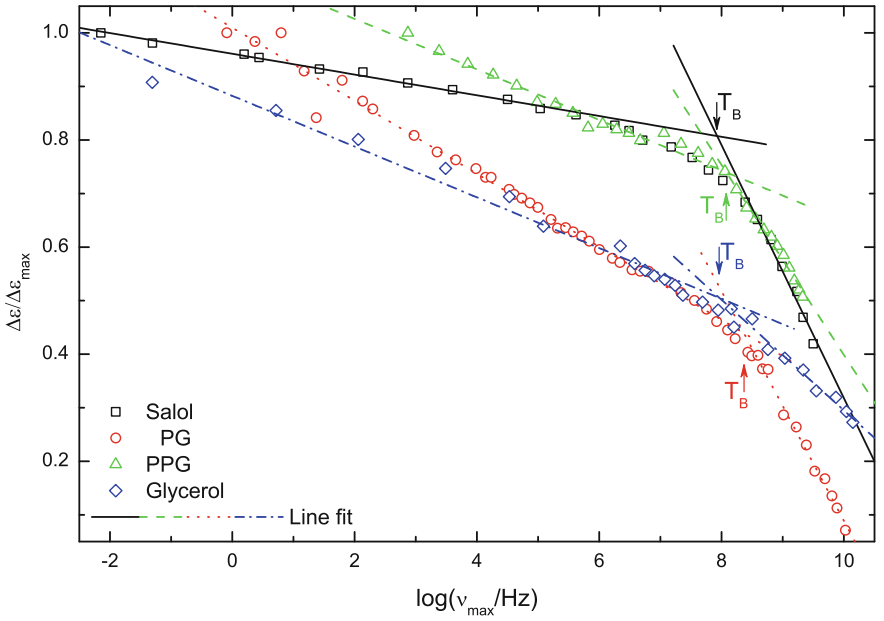

Fig. 8 Relaxational strength $\Delta\varepsilon$, normalized with its maximum value versus the mean relaxation rate log ν_{max} for salol, propylene glycol (PG), poly(propylene glycol) (PPG) and glycerol as indicated. At the temperature T_B, the slope of the correlation between $\Delta\varepsilon$ and ν_{max} changes. The data for salol are taken from [22], for PG and PPG from [16] and for glycerol from [81]

$$\omega_{\min} \sim \left|\frac{T - T_c}{T_c}\right|^{\frac{1}{2a}} \tag{27}$$

$$\omega_{\max} \sim \left|\frac{T - T_c}{T_c}\right|^{\left(\frac{1}{2a}+\frac{1}{2b}\right)} \tag{28}$$

Carrying out such an analysis delivers for glycerol a value of $a = 0.325$ and $b = 0.63$. For the lowest temperatures, the increase towards the boson peak approaches a power law $\varepsilon'' \sim \nu^3$ as indicated by the dashed line in Fig. 9. The inset demonstrates for two temperatures that the simple superposition ansatz of, Eq. (25), is not sufficient to describe the shallow minimum.

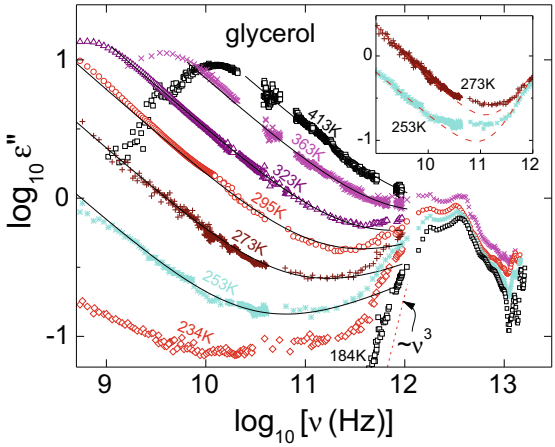

Fig. 9 Dielectric loss of glycerol in the minimum and boson peak region. The solid lines are fits with the MCT prediction, Eq. (10), with $a = 0.325$, $b = 0.63$ for glycerol. For the lowest temperatures, the increase towards the boson peak approaches power laws $\varepsilon \sim \nu^3$ for glycerol as indicated by the dashed line. Note that, in contrast to PC, the boson peak seems to be superimposed to the shallow minimum in glycerol. The inset demonstrates for two temperatures that the simple superposition ansatz, Eq. (9), is not sufficient to explain the shallow minimum. Taken from [82] with permission

4 Conclusions

In the spectral range between 10^{-3} and 10^{13} Hz, four dynamic processes take place in the dynamic glass transition, slow and fast secondary relaxations and the boson-peak. The questions formulated in the introduction can be answered in detail:

(i) Is there a scaling function which describes the temperature dependence of the mean relaxation rate in the entire spectral range from 10^{+13} to 10^{-3} Hz and below?
For all materials under study, *none* of the suggested scaling functions is able to describe the observed temperature dependence of the mean relaxation rate in the entire spectral range. The analysis of the data using derivative plots reveals furthermore, that even in the high-frequency limit an Arrhenius dependence does not describe the measurements within the limits of experimental accuracy. The empirical Vogel–Fulcher–Tammann dependence turns out to be a coarse-grained description only within a limited temperature range. There is no indication pointing towards a divergence at the Vogel temperature T_0.

(ii) How does the relaxation time distribution function change with temperature or in other words, is time–temperature superposition in general valid for (dielectric) relaxation processes?
The relaxation time distribution function with its shape parameters β and γ shows a pronounced temperature dependence. Hence, time–temperature superposition is *not* valid in general.

(iii) How does the strength $\Delta\varepsilon$ of a relaxation process change with temperature in the course of the dynamic glass transition?
The relaxation strength $\Delta\varepsilon$ of the dynamic glass transition decreases with increasing temperature, an effect which can be not explained by the temperature dependence of the density. Instead an increasing length scale of the dynamic glass transition seems to be likely resulting in an increased effective dipole moment.

(iv) What is the molecular origin of the "high-frequency" wing which is observed in the dynamic glass transition of many (low molecular weight and polymeric) systems?
Several glass formers show a high-frequency wing; it is considered as a slow secondary relaxation which might be coupled to the dynamic glass transition.

(v) What is the assignment of the "fast secondary relaxation"?
In the spectral range between 10^9 and 10^{12} Hz, a fast secondary relaxation is observed. It can be quantitatively described by the MCT.

(vi) Is there a characteristic temperature, where glassy dynamics undergoes a change?
As suggested by A. Schönhals, one observes by displaying the correlation between the two dependent variables, relaxation strength and mean relaxation rate—without any assumptions—a transition at about 10^8 Hz. This might be interpreted as the onset of cooperative dynamics with decreasing temperature.

Acknowledgements Support by M. Anton in preparing some of the figures is highly acknowledged.

References

1. 1th international discussion meeting on relaxation in complex systems. J Non-Cryst Solids 131–133:1–1285 (1991); 2th international discussion meeting on relaxation in complex systems. J Non-Cryst Solids 172–174:1–1457 (1994); 3th international discussion meeting on relaxation in complex systems. J Non-Cryst Solids 235–237:1–814 (1998); 4th international discussion meeting on relaxation in complex systems. J Non-Cryst Solids 307–310:1–1080 (2002); 5th international discussion meeting on relaxation *in* complex systems. J Non-Cryst Solids 352:4731–5250 (2006); 6th international discussion meeting *on r*elaxation in *c*omplex systems. J Non-Cryst Solids 357:241–782 (2011); 7th international discussion meeting on *r*elaxation in *c*omplex systems (2013); 8th international discussion meeting on relaxation in complex systems (2017)
2. Wong J, Angell CA (1976) Glass: structure by spectroscopy. Marcel Dekker, New York
3. Donth EJ (1981) Glasübergang. Akademie Verlag, Berlin
4. Zallen R (1983) The physics of amorphous solids. Wiley, New York
5. Elliott SR (1990) Physics of amorphous materials. Longman Scientific & Technical, London
6. Donth EJ (1992) Relaxation and thermodynamics in polymers, glass transition. Akademie Verlag, Berlin
7. Donth EJ (2001) The glass transition. Springer, Berlin
8. Ngai K (2011) Relaxation and diffusion in complex systems. Springer, Berlin
9. Götze W (2012) Complex dynamics of glass-forming liquids—a mode-coupling theory. Oxford Scientific Publications, Oxford

10. Cheng SZD (ed) (2002) Handbook of thermal analysis and calorimetry. Elsevier Science B.V
11. Hecksher T, Torchinsky DH, Klieber C, Johnson JA, Dyre JC, Nelson KA (2017) PNAS 114:8715
12. Jeon YH, Nagel SR, Bhattacharya S (1986) Phys Rev A 34:602
13. Pecora R (ed) (1985) Dynamic light scattering, applications of photon correlation spectroscopy. Springer
14. Frick B, Richter D (1995) Science 267:1939–1945
15. Schmidt-Rohr K, Spiess HW (1994) Multidimensional solid-state NMR and polymers. Academic Press, London
16. Kremer F, Schönhals A (eds) (2003) Broadband dielectric spectroscopy. Springer
17. Williams G, Watts DC (1970) Trans Faraday Soc 66:80
18. Williams G, Watts DC, Dev SB, North AM (1971) Trans Faraday Soc 67:1323
19. Johari GP, Goldstein M (1970) J Chem Phys 53:2372
20. Johari GP (1976) In: Goldstein M, Simha R (eds) The glass transition and the nature of the glassy state. Ann New York Acad Sci 279:117
21. Johari GP (1986) J Chem Phys 85:6811
22. Dixon PK, Wu L, Nagel SR, Williams BD, Carini JP (1990) Phys Rev Lett 65:1108
23. Dixon PK (1990) Phys Rev B 42:8179
24. Dixon PK, Menon N, Nagel SR (1994) Phys Rev E 50:1717
25. Lunkenheimer P, Gerhard G, Drexler F, Böhmer R, Loidl A (1995) Z Naturforsch 50A:1151
26. Lunkenheimer P, Pimenov A, Schiener B, Böhmer R, Loidl A (1996) Europhys Lett 33:611
27. Lunkenheimer P, Loidl A (1996) J Chem Phys 104:4324
28. Lunkenheimer P, Pimenov A, Dressel M, Gonscharev Yu G, Böhmer R, Loidl A (1996) Phys Rev Lett 77:318
29. Lunkenheimer P, Pimenov A, Loidl A (1997) Phys Rev Lett 78:2995
30. Lunkenheimer P, Pimenov A, Dressel M, Schiener B, Schneider U, Loidl A (1997) Progr Theor Phys Suppl 126:123
31. Lunkenheimer P, Schneider U, Brand R, Loidl A (1999) In: Tokuyama M, Oppenheim I (eds) Slow dynamics in complex systems: Eighth Tohwa University International Symposium. AIP, New York, AIP Conf Proc 469:433
32. Schönhals A, Kremer F, Schlosser E (1991) Phys Rev Lett 67:999
33. Schönhals A, Kremer F, Hofmann A, Fischer EW, Schlosser E (1993) Phys Rev Lett 70:3459
34. Schönhals A, Kremer F, Stickel F (1993) Phys Rev Lett 71:4096
35. Schönhals A, Kremer F, Schlosser E (1993) Progr Colloid Polym Sci 91:39
36. Schönhals A, Kremer F, Hofmann A, Fischer EW (1993) Phys A 201:263
37. Stickel F, Fischer EW, Schönhals A, Kremer F (1994) Phys Rev Lett 73:293632, b. Stickel F, Fischer EW, Richert R (1995) J Chem Phys 102:6521
38. Hofmann A, Kremer F, Fischer EW, Schönhals A (1994) In: Richert R, Blumen A (eds) Disorder effects on relaxational processes. Springer, Berlin, Chap. 10:309
39. Vogel H (1921) Phys Z 22:645
40. Fulcher GS (1923) J Am Ceram Soc 8:339
41. Tammann G, Hesse W (1926) Z Anorg Allg Chem 156:245
42. Angell CA (1985) In: Ngai KL, Wright GB (eds) Relaxations in complex systems. NRL, Washington, DC: 3
43. Kauzmann W (1942) Rev Mod Phys 14:12
44. Kauzmann W (1948) Chem Rev 43:219
45. Gibbs JH, DiMarzio EA (1958) J Chem Phys 28:373
46. Hecksher T, Nielsen AI, Olsen NB, Dyre JC (2008) Nat Phys 4(9):737–741
47. Davidson DW, Cole RH (1951) J Chem Phys 19:1484
48. Poley JPh (1955) J Appl Sci B4:337
49. Angell CA (1997) Physica D 107:122
50. Stillinger FH (1995) Science 267:1935
51. Debenedetti PG, Stillinger FH (2000) Nature 410:259
52. Adam G, Gibbs JH (1965) J Chem Phys 43:139

53. Doolittle AK (1951) J Appl Phys 22:1471
54. Cohen MH, Turnbull D (1959) J Chem Phys 31:1164
55. Cohen MH, Grest GS (1979) Phys Rev B 20:1077
56. Donth E, Hempel E, Schick Ch (2000) J Phys Cond Mat 12:L281
57. Donth E, Huth H, Beiner M (2001) J Phys: Cond Mat 13:L451
58. Kirkpatrick TR, Tirumalai D (1989) Phys Rev A 40:1045
59. Waterton SCJ (1932) Soc Glass Technol 16:244
60. Mauro JC, Yue Y, Ellison AJ, Gupta PK, Allan DC (2009) PNAS 106(47):19780–19784
61. Souletie H, Bertrand D (1991) J Phys (Paris) 51:1627
62. Dyre JC (2006) Rev Mod Phys 78(3):953–972
63. Dyre JC, Olsen NB (2004) PRE 69:042501
64. Dyre JC, Olsen NB, Christensen T (1996) PRB 53:2171
65. Hecksher T, Dyre JC (2015) J Non-Cryst Solids 407:14
66. Leutheuser E (1984) Phys Rev A 29:2765
67. Bengtzelius U, Götze W, Sjölander A (1984) J Phys C 17:5915
68. Götze W (1985) Z Phys B 60:195
69. Götze W, Sjögren L (1992) Rep Prog Phys 55:241
70. Bartoš J, Iskrová M, Köhler M, Wehn R, Šauša O, Lunkenheimer P, Krištiak J, Loidl A (2011) Eur Phys J E 34:104
71. Schneider U, Brand R, Lunkenheimer P, Loidl A (2000) PRL 84:5560
72. Lunkenheimer P, Wehn R, Riegger Th, Loidl A (2002) J Non-Cryst Solids 307–310:336–344
73. Lunkenheimer P, Schneider U, Brand R, Loidl A (2000) Contemp Phys 41:15
74. Novikov VN, Sokolov AP (2015) PRE 92:062304
75. Lunkenheimer P, Kastner S, Köhler M, Loidl A (2010) PRE 81:051504
76. Lunkenheimer P, Wehn R, Köhler M, Loidl A (2018) J Non-Cryst Solids 492:63
77. Schönhals A (1995) Habilitation thesis. Technical University Berlin
78. Hofmann A (1993), Dissertation, University Mainz
79. Schönhals A (2001) EPL 56:815–821
80. Kremer F (ed) (2014) Dynamics in geometrical confinement. Springer, Berlin
81. Lunkenheimer P, Loidl A (2002) Chem Phys 284:205–219
82. Lunkenheimer P, Loidl A (2002) Glassy dynamics beyond the alpha-relaxation. In: Kremer F, Schönhals A (eds) Broadband Dielectric Spectroscopy. Springer, Berlin Chapter 5